Electronic Supplementary Material (ESI) for Journal of Materials Chemistry C.

Supporting Information

Engineering Functionalized Low LUMO [1]Benzothieno[3,2-*b*][1]benzothiophenes (BTBTs): Unusual Molecular and Charge Transport Properties

Resul Ozdemir,[†1] *Kyunghan Ahn,*[†2] *İbrahim Deneme,*[1] *Yunus Zorlu,*[3] *Dojun Kim,*[2]

Myung-Gil Kim,[2] *Hakan Usta*[1*]

[1] Department of Materials Science and Nanotechnology Engineering, Abdullah Gül University, Kayseri 38080, Turkey.

[2] School of Advanced Materials Science & Engineering, Sungkyunkwan University, Suwon 2066 Republic of Korea.

[3] Department of Chemistry, Gebze Technical University, Gebze, Kocaeli 41400, Turkey.

*Address correspondence to: hakan.usta@agu.edu.tr

† These authors contributed equally to this work.

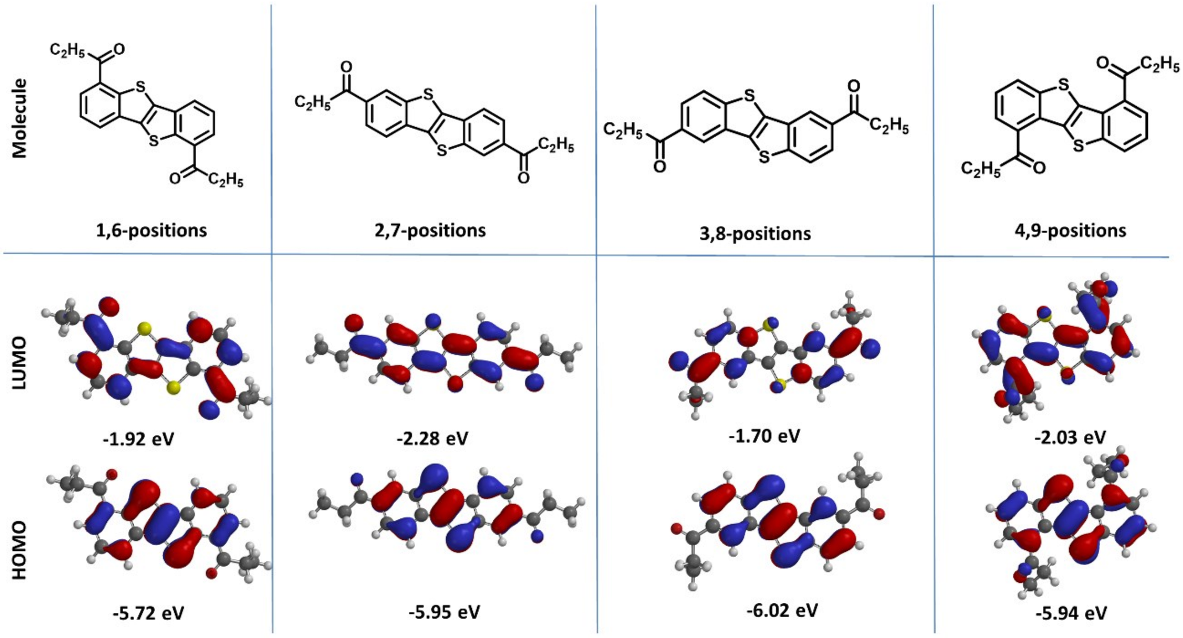

Figure S1. Theoretical (DFT/B3LYP/6-31G**) HOMO/LUMO energy levels of **D(C_7CO)-BTBT** along with topographical orbital representations for different functionalization positions.

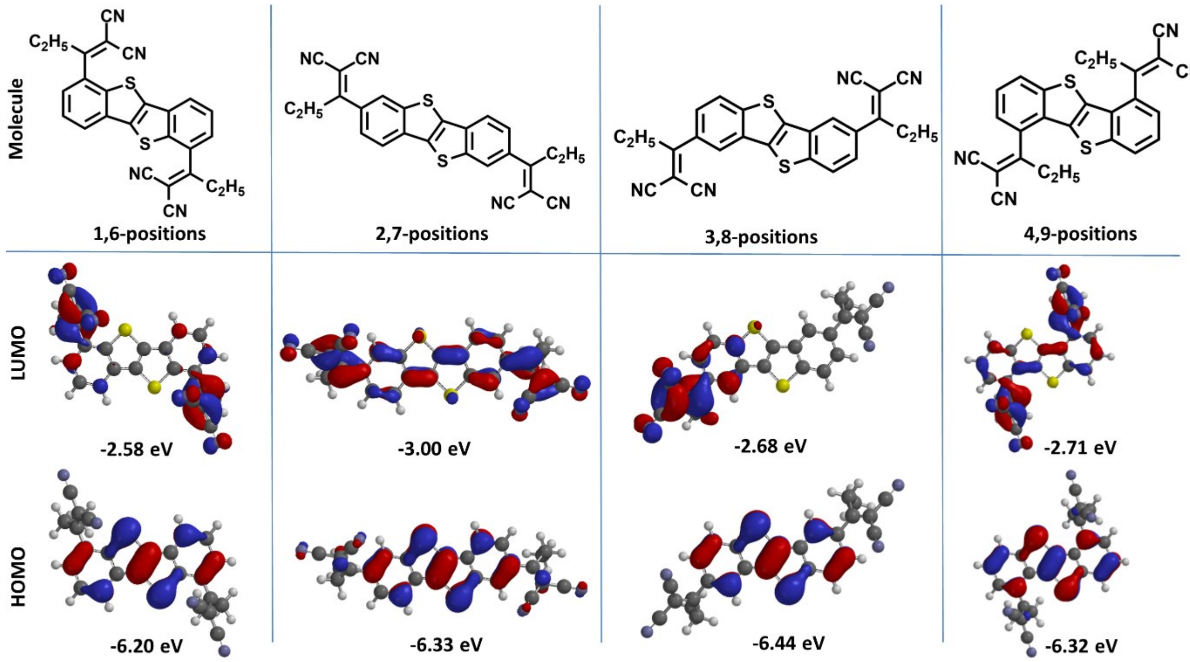

Figure S2. Theoretical (DFT/B3LYP/6-31G**) HOMO/LUMO energy levels of **D(C_7CC(CN)$_2$)-BTBT** along with topographical orbital representations for different functionalization positions.

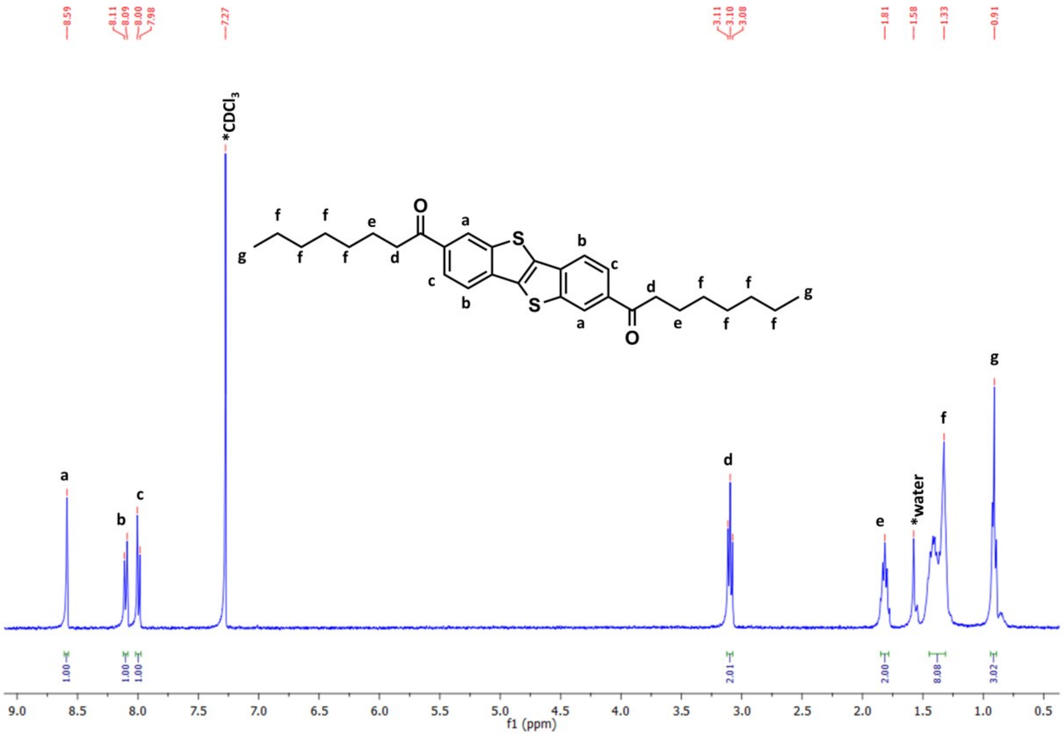

Figure S3. ^{1}H NMR spectra of **D(C$_7$CO)-BTBT** measured in CDCl$_3$.

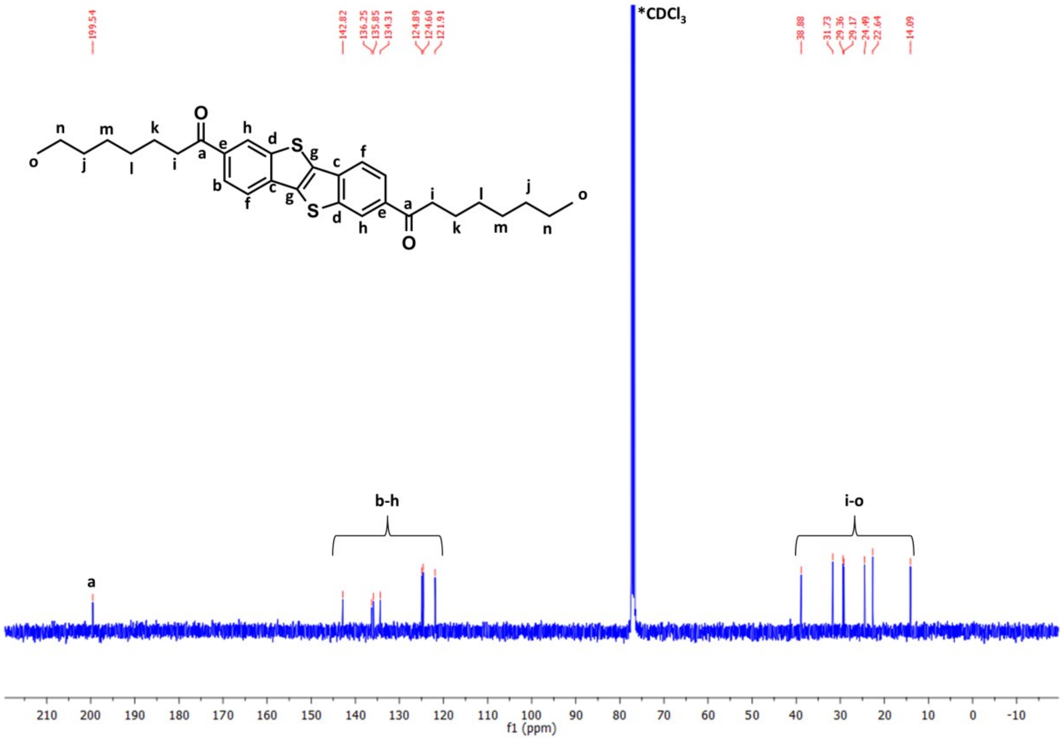

Figure S4. ^{13}C NMR spectra of **D(C$_7$CO)-BTBT** measured in CDCl$_3$.

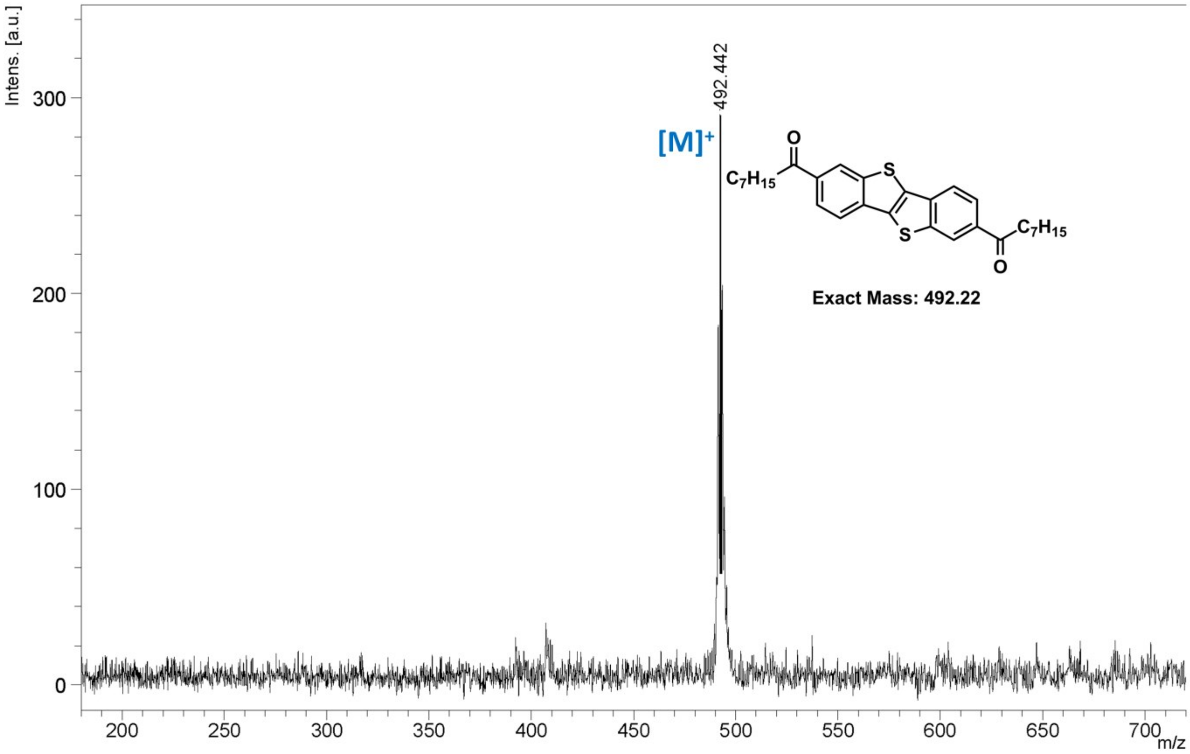

Figure S5. Positive ion and linear mode MALDI TOF-MS spectrum of **D(C_7CO)-BTBT**.

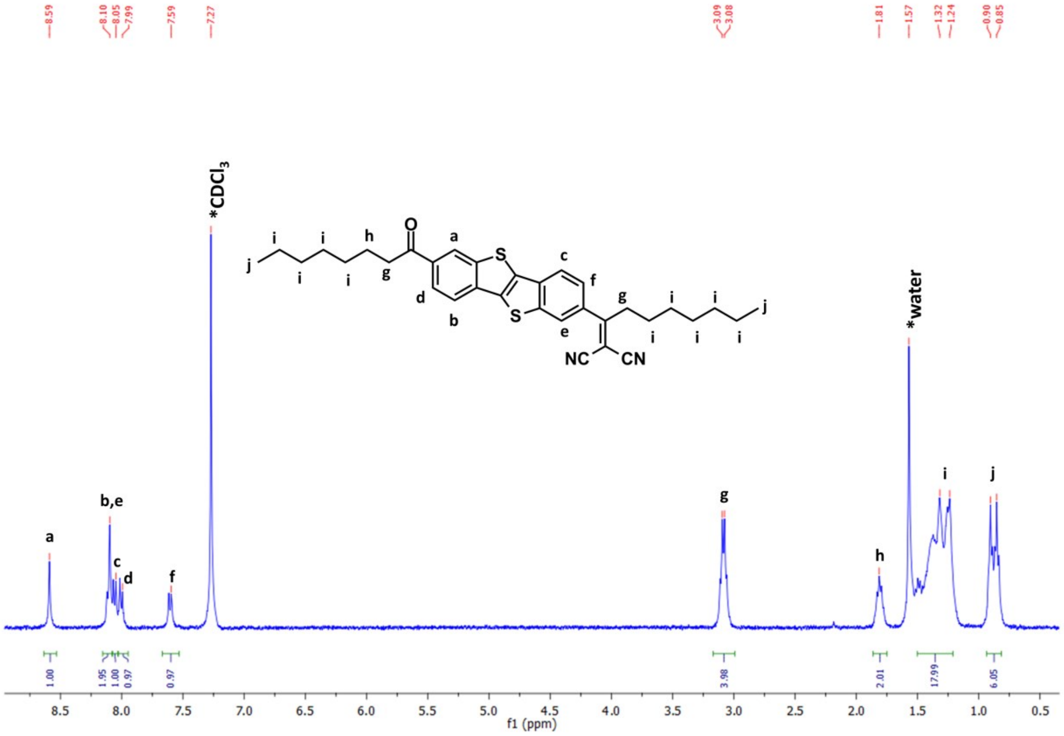

Figure S6. ^{1}H NMR spectra of **C_7CO-BTBT-CC(CN)$_2C_7$** measured in $CDCl_3$.

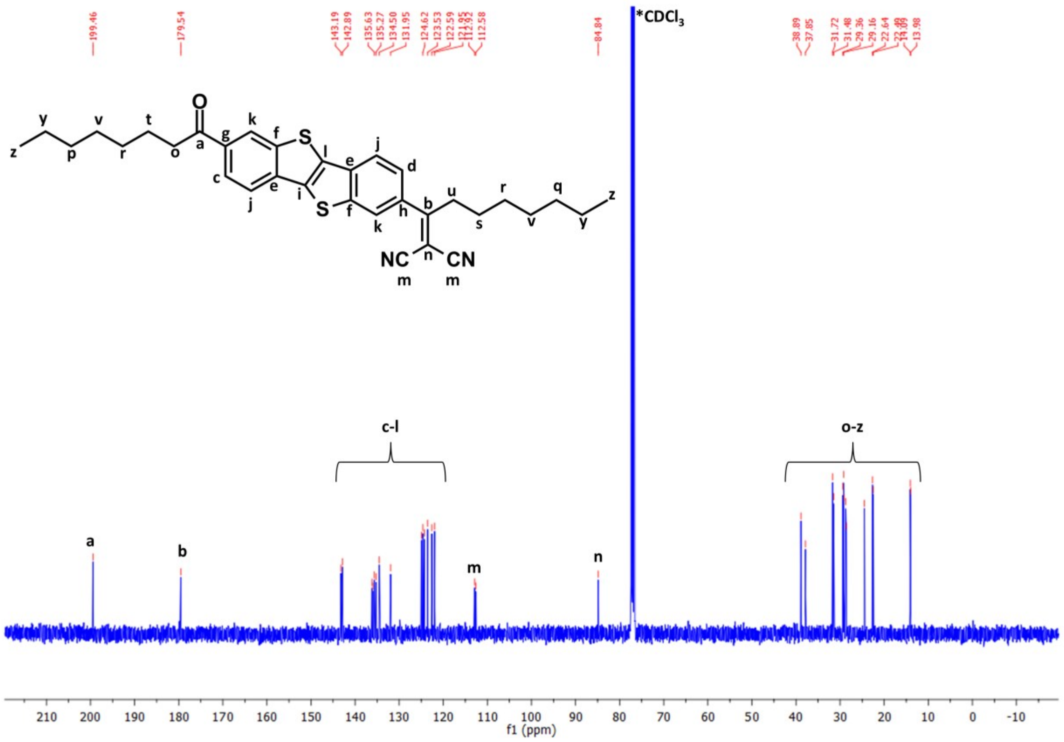

Figure S7. ^{13}C NMR spectra of **C_7CO-BTBT-CC(CN)$_2$$C_7$** measured in $CDCl_3$.

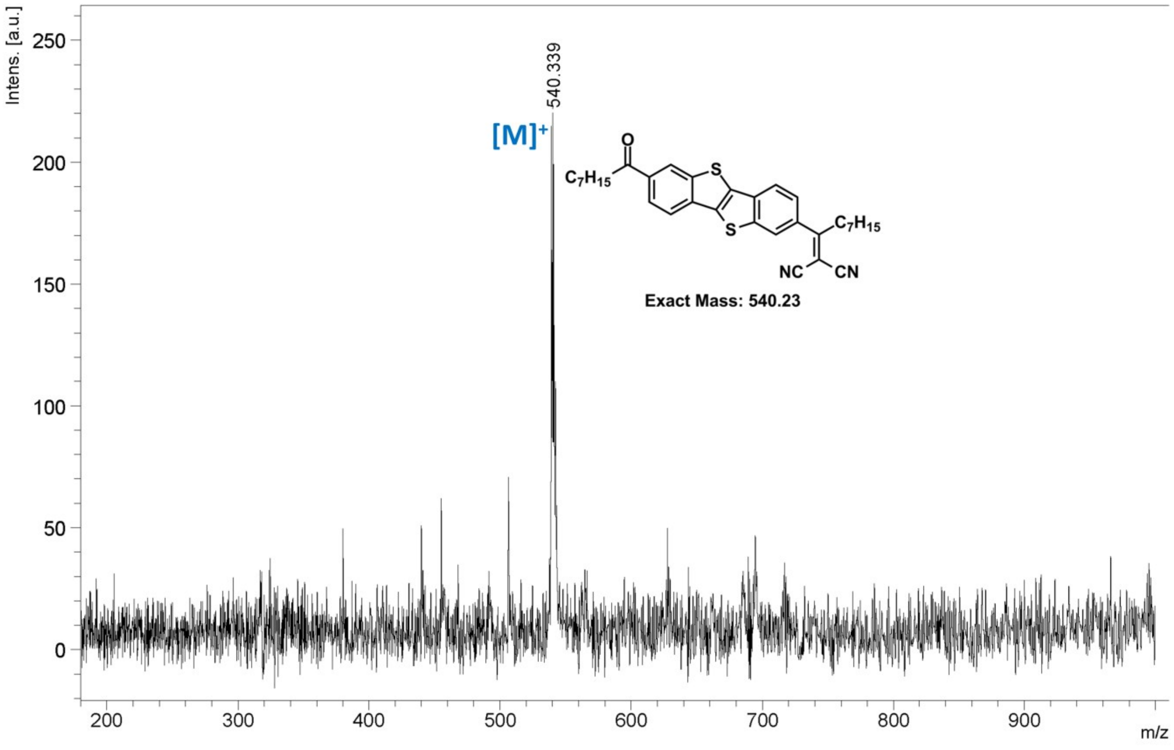

Figure S8. Positive ion and linear mode MALDI TOF-MS spectrum of **C_7CO-BTBT-CC(CN)$_2$$C_7$**.

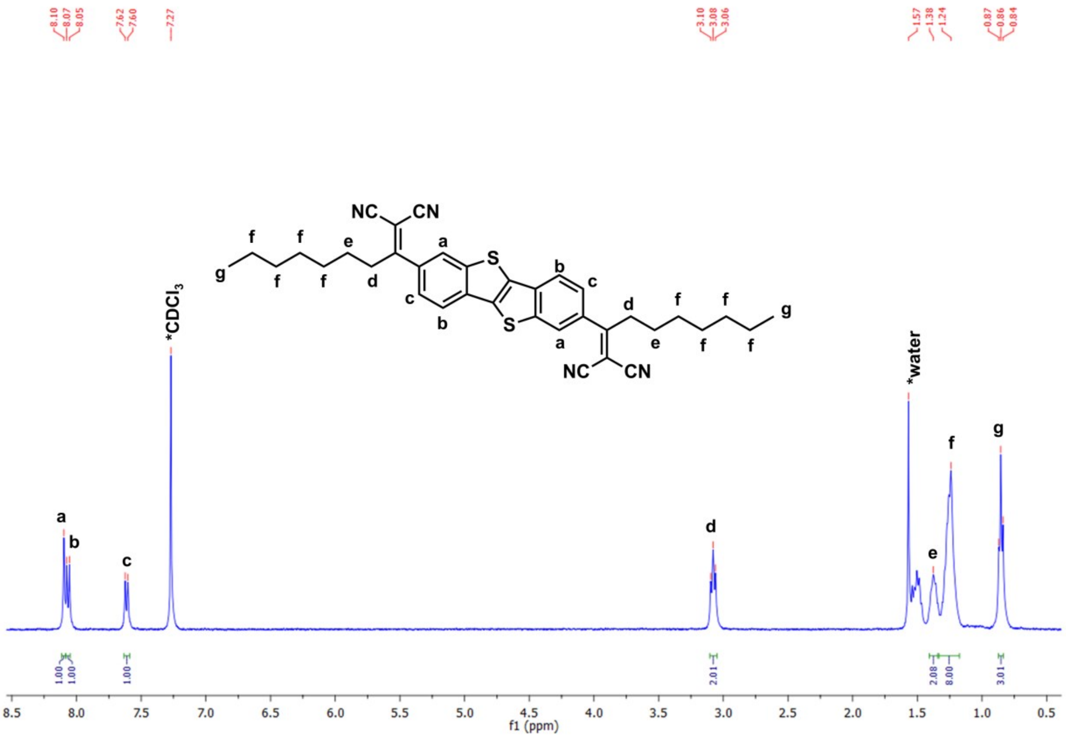

Figure S9. ^{1}H NMR spectra of **D(C$_7$CC(CN)$_2$)-BTBT** measured in CDCl$_3$.

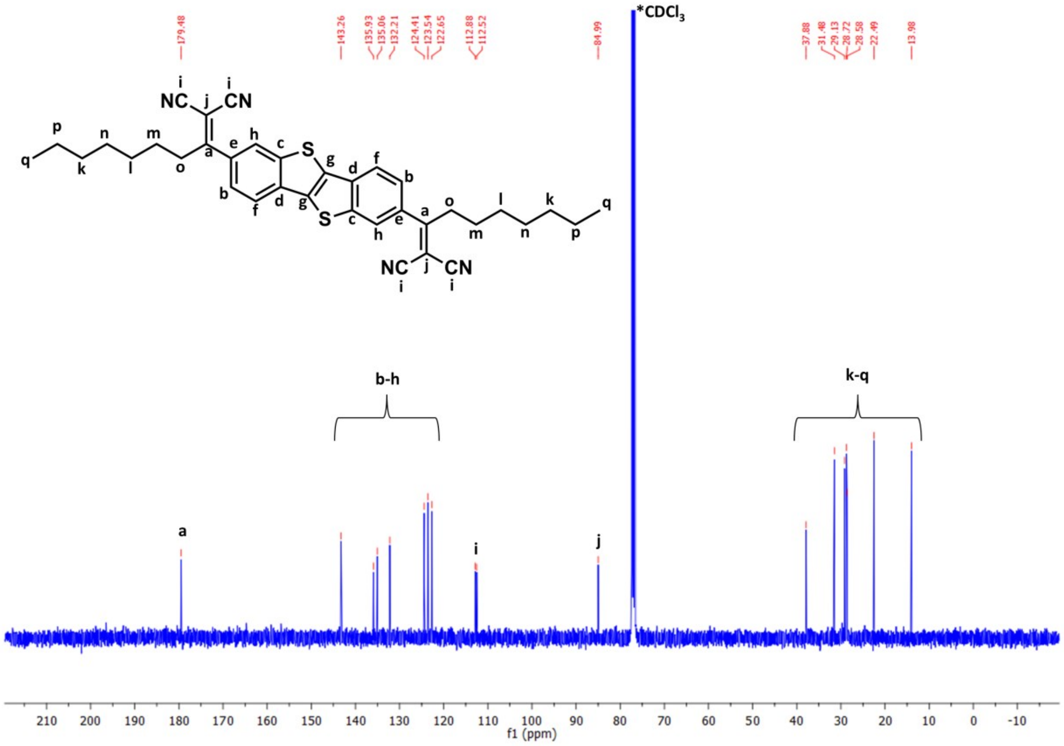

Figure S10. ^{13}C NMR spectra of **D(C$_7$CC(CN)$_2$)-BTBT** measured in CDCl$_3$.

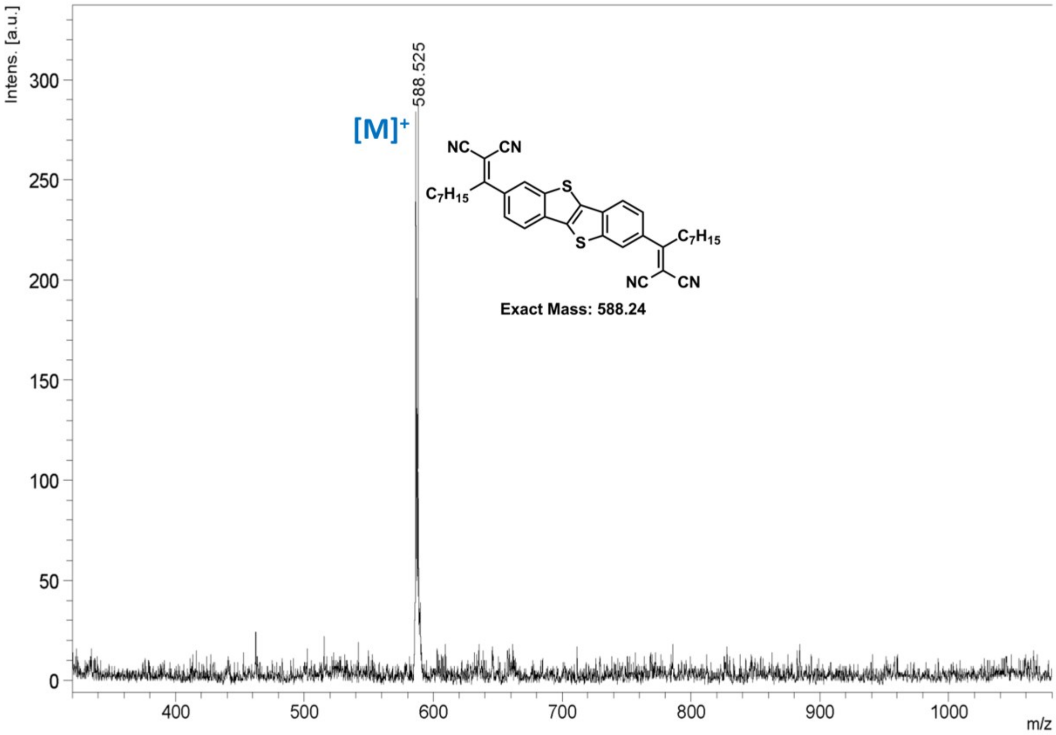

Figure S11. Positive ion and linear mode MALDI TOF-MS spectrum of **D(C_7CC($CN)_2$)-BTBT**.

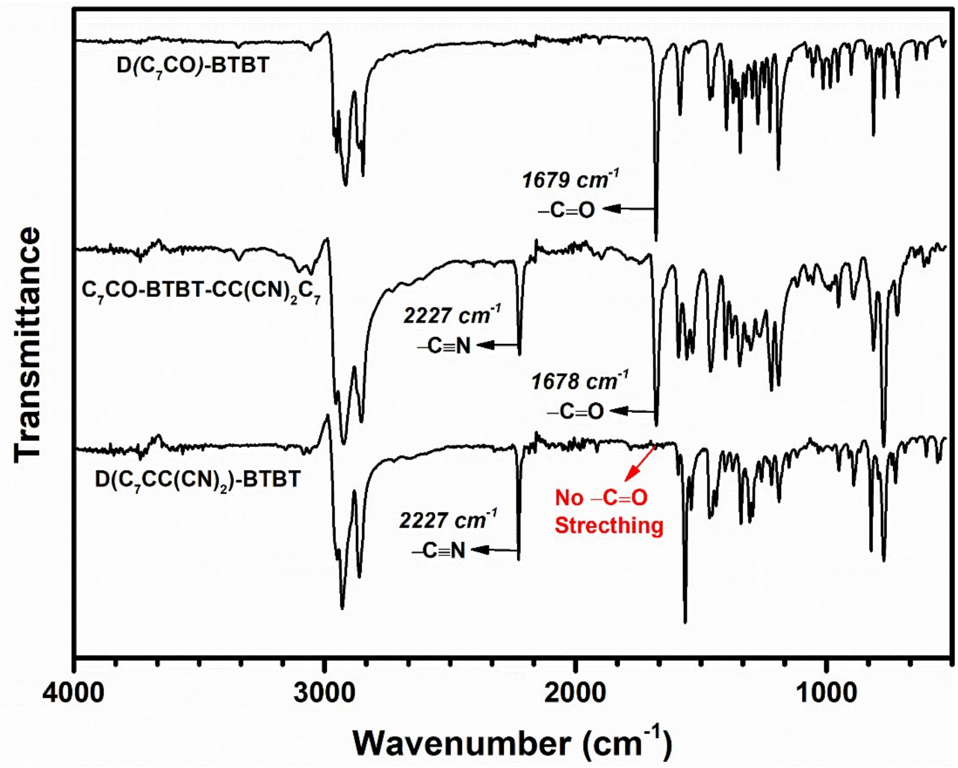

Figure S12. FT-IR spectra of **D(C_7CO)-BTBT**, **C_7CO-BTBT-CC($CN)_2C_7$**, and **D(C_7CC($CN)_2$)-BTBT** showing C=O (1680 cm^{-1}) and C≡N (2227 cm^{-1}) stretching vibrational peak.

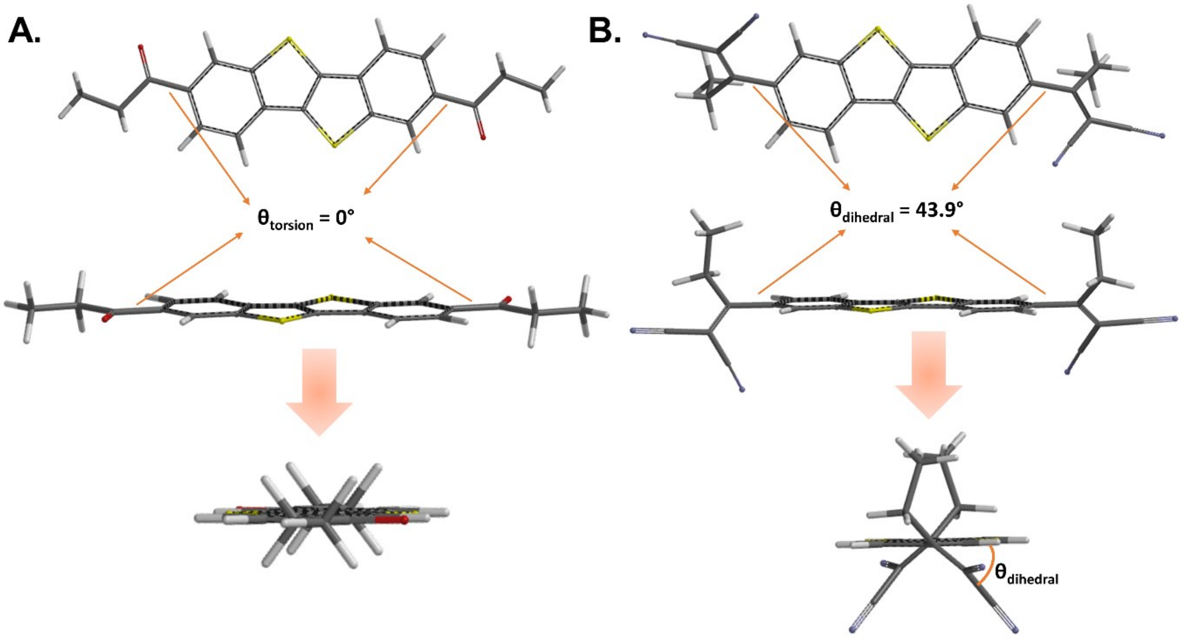

Figure S13. Computationally optimized (DFT/B3LYP/6-31G**) molecular structures for **D(C_7CO)-BTBT** (A) and **D(C_7CC(CN)$_2$)-BTBT** (B) showing the torsion and dihedral angles ($\theta_{torsion}$ and $\theta_{dihedral}$) between BTBT π-system and carbonyl/dicyanovinylene functional groups.

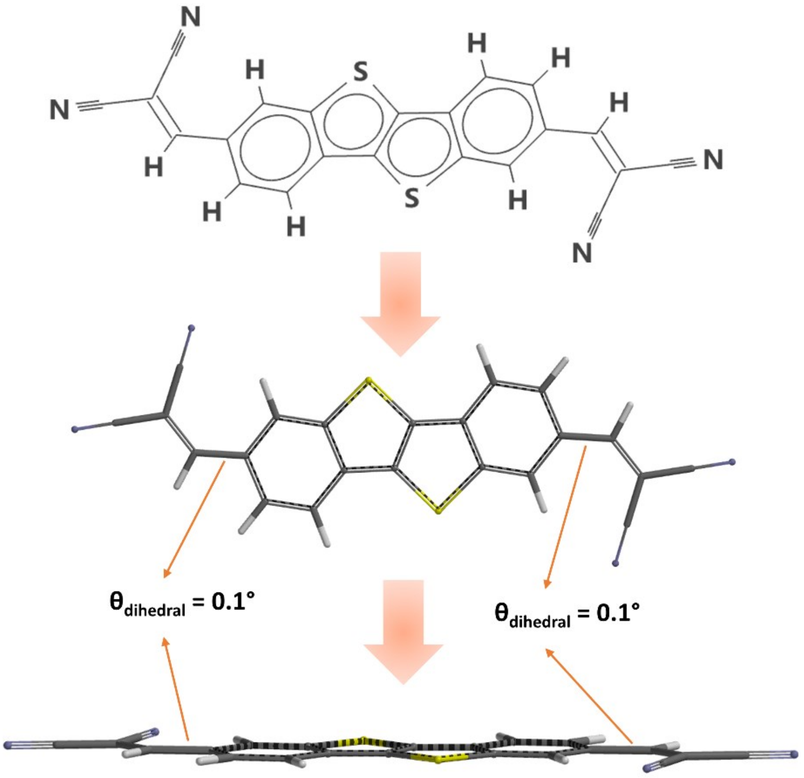

Figure S14. Computationally optimized (DFT/B3LYP/6-31G**) molecular structure of a hypothetical dicyanovinylene-functionalized BTBT compound, **D(HCC(CN)$_2$)-BTBT**, showing the dihedral angle ($\theta_{dihedral}$) between BTBT π-system and dicyanovinylene functional groups.

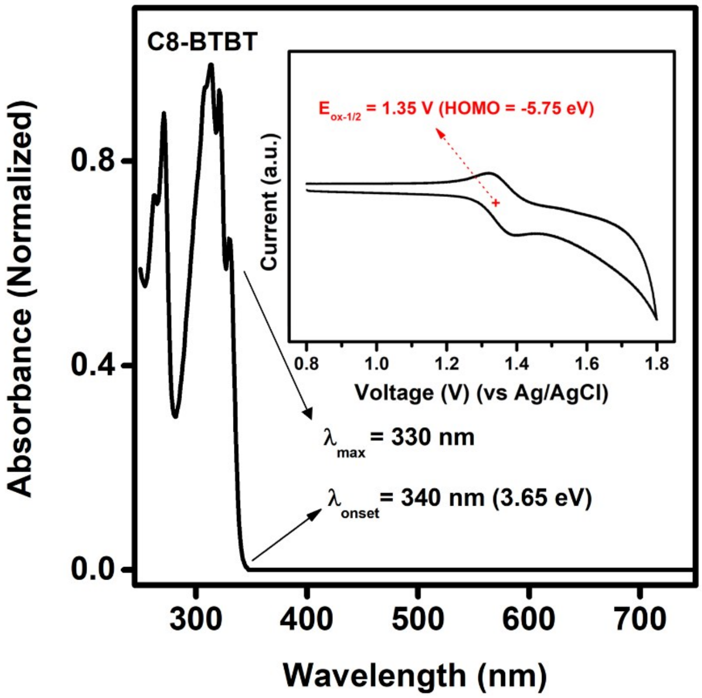

Figure S15. Optical absorption spectrum and cyclic voltammogram (0.1 M $Bu_4N^+PF_6^-$, scan rate = 50 mV/s) of **C_8-BTBT** in dichloromethane solutions.

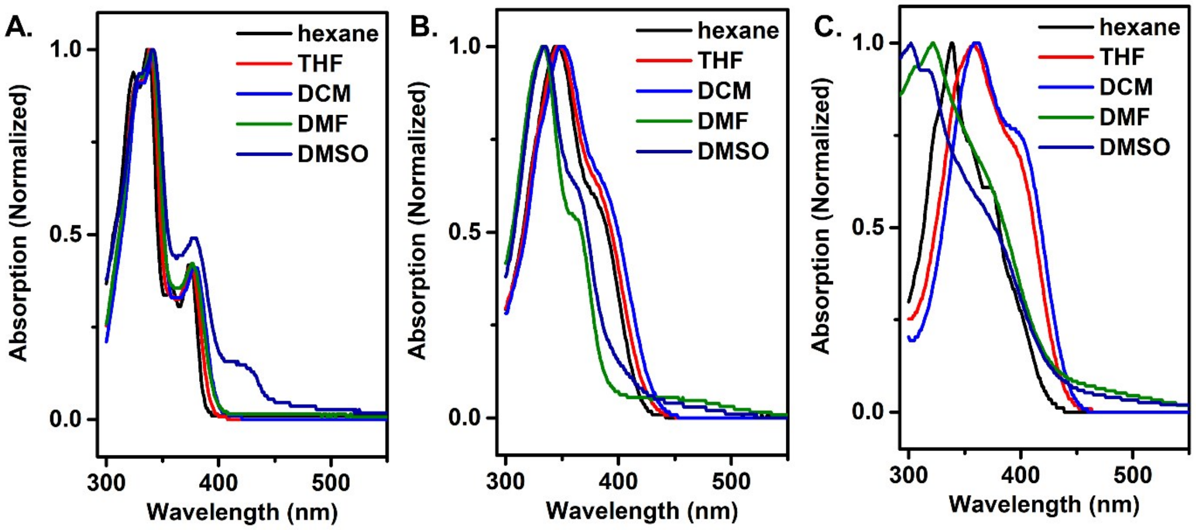

Figure S16. Optical absorption spectra of **D(C_7CO)-BTBT** (A), **C_7CO-BTBT-CC(CN)$_2$$C_7$** (B), and **D($C_7$CC(CN)$_2$)-BTBT** (C) in hexane, tetrahydrofuran (THF), dichloromethane (DCM), N,N'-dimethylformamide (DMF), and dimethyl sulfoxide (DMSO).

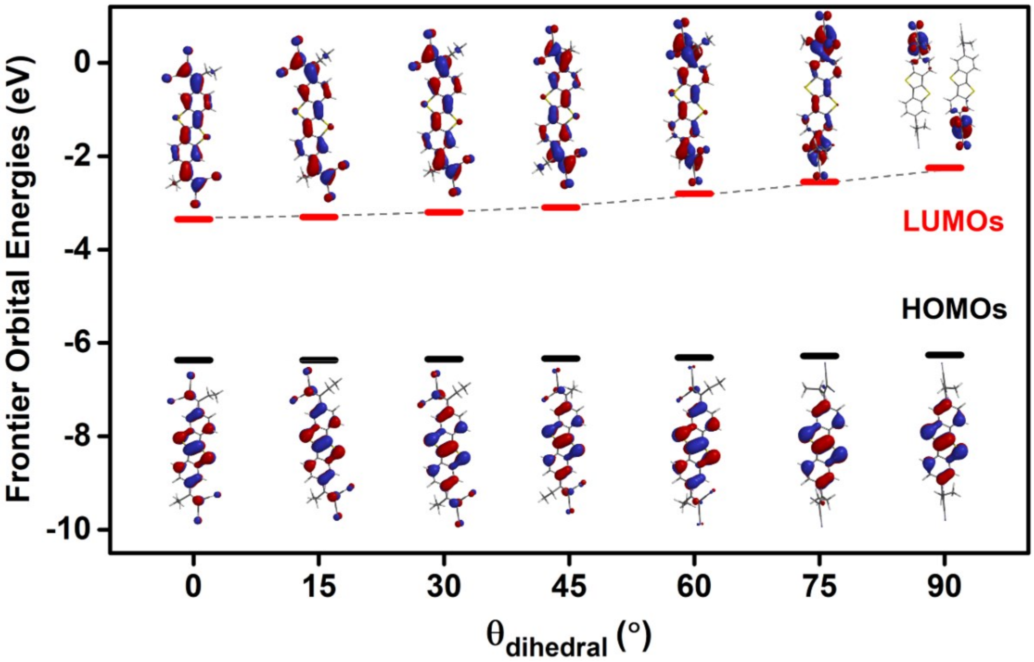

Figure S17. Theoretical (DFT/B3LYP/6-31G**) frontier orbital energies along with topographical representations for conformations of **D(C_7CC(CN)$_2$)-BTBT** with varied dihedral angles ($\theta_{dihedral}$) between the BTBT π-system and dicyanovinylene units.

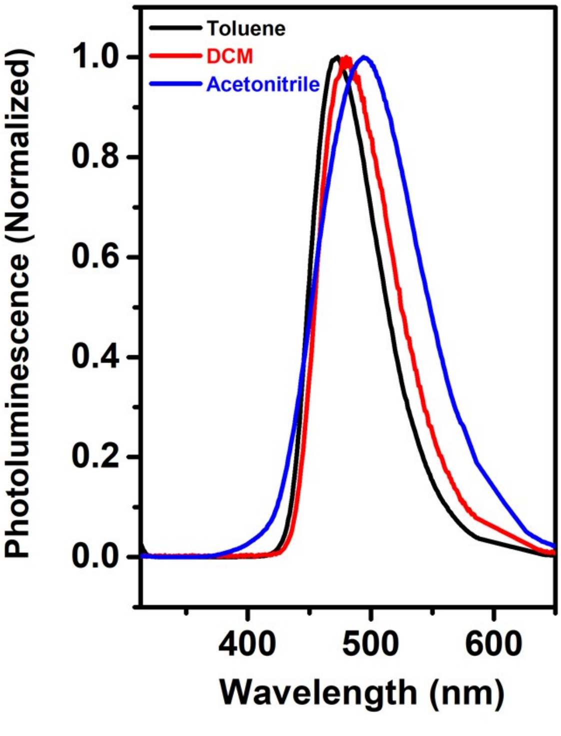

Figure S18. The solvent polarity-dependent (toluene (f (ε,n) = 0.014) → dichloromethane (f (ε,n) = 0.217) → acetonitrile (f (ε,n) = 0.305)) photoluminescence spectra of **D(C_7CC(CN)$_2$)-BTBT** (λ_{exc} = 405 nm) in solution (1.0×10^{-5} M).

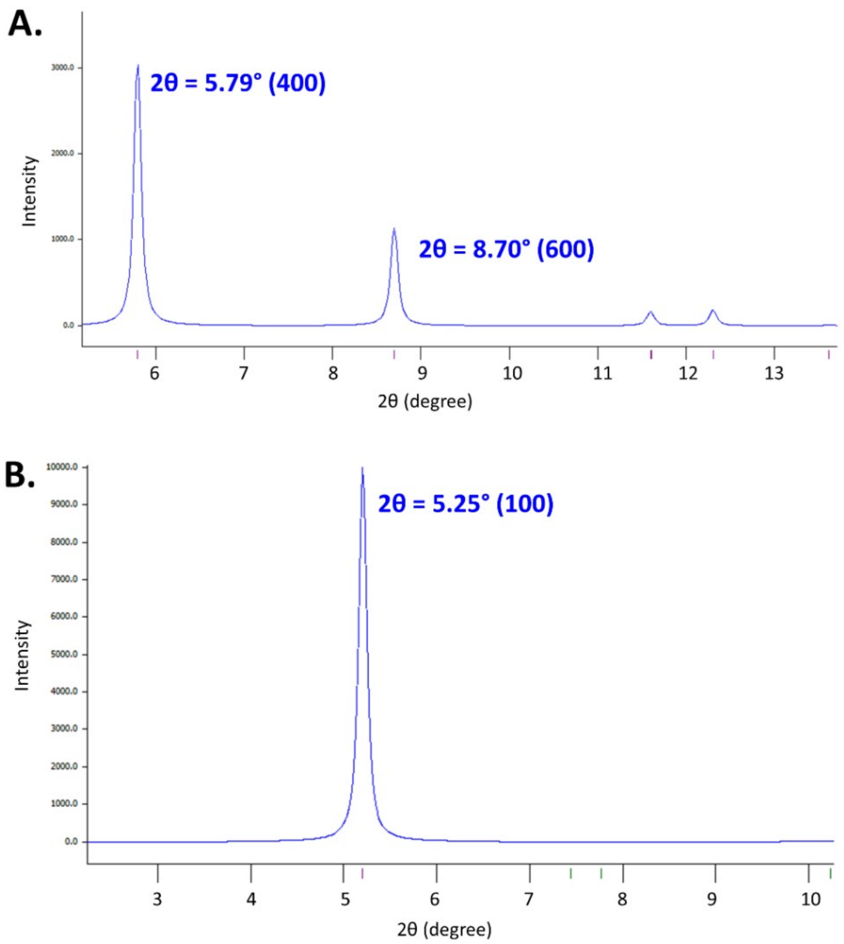

Figure S19. Simulated XRD powder patterns based on the single-crystal structures for **D(C$_7$CO)-BTBT** (A) and **D(C$_7$CC(CN)$_2$)-BTBT** (B) indicating the selected matching diffraction peaks and lattice planes at 2θ = 5.79(400)/8.70˚(600) and at 2θ = 5.25˚(100), respectively.

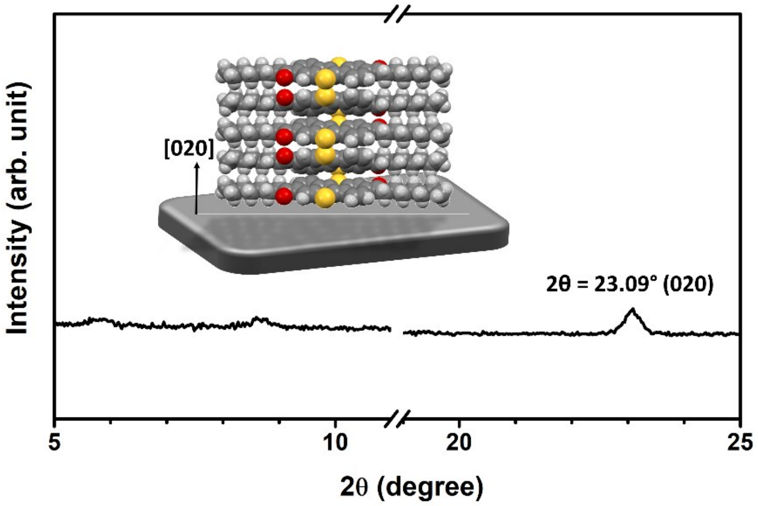

Figure S20. Grazing incidence X-ray diffraction (GIXD) of **D(C$_7$CO)-BTBT** (30 nm) thin film deposited on n^{++}-Si/SiO$_2$(200 nm)/HMDS substrate at a deposition temperature of 25 °C and the corresponding (020) lattice plane/molecular arrangement.

X-ray data collection and structure refinement

Data were obtained with Bruker APEX II QUAZAR three-circle diffractometer. Indexing was performed using APEX2 [APEX2, version 2014.11-0, Bruker (2014), Bruker AXS Inc., Madison, WI]. Data integration and reduction were carried out with SAINT [SAINT, version 8.34A, Bruker (2013), Bruker AXS Inc., Madison, WI]. Absorption correction was performed by multi-scan method implemented in SADABS [SADABS, version2014/5, Bruker (2014), Bruker AXS Inc., Madison, WI]. The structure was solved using SHELXT[1] and then refined by full-matrix least-squares refinements on F^2 using the SHELXL[2] in Olex2 Software Package[3]. For **D(C_7CO)-BTBT** single crystals obtained was very thin size (0.12 mm × 0.04 mm × 0.03 mm), even with high exposure times (second/frame) is used, they were obviously very weakly diffracting crystals, and it could not be obtained the intensity of higher angle diffraction signals (d = 0.77 Å, $2\Theta = 55^o$) in the diffraction pattern, which lowered the completeness of higher angle data (completeness of **D(C_7CO)-BTBT** is only 0.945). In our study, in order to improve the crystal quality of **D(C_7CO)-BTBT**, we made a large number of crystallization experiments and the most ideal single crystal was reported in this study. Aromatic C-bound H atoms were positioned geometrically and refined using a riding mode. Crystallographic data and refinement details of the data collection for **D(C_7CO)-BTBT** and **D(C_7CC$(CN)_2$)-BTBT** are given in Table S1. Crystal structure validations and geometrical calculations were performed using Platon software[4]. Mercury software[5] was used for visualization of the cif files. Additional crystallographic data with CCDC reference numbers (1946322 for **D(C_7CO)-BTBT** and 1946323 for **D(C_7CC$(CN)_2$)-BTBT**) have been deposited within the Cambridge Crystallographic Data Center via www.ccdc.cam.ac.uk/deposit.

Table S1. Crystal data and refinement parameters for **D(C$_7$CO)-BTBT** and **D(C$_7$CC(CN)$_2$)-BTBT**.

	D(C$_7$CO)-BTBT	**D(C$_7$CC(CN)$_2$)-BTBT**
CCDC	1946322	1946323
Empirical Formula	$C_{30}H_{36}O_2S_2$	$C_{36}H_{36}N_4S_2$
Formula weight (g. mol^{-1})	492.71	588.81
Temperature (K)	296.15	296.15
Wavelength (Å)	MoK$_\alpha$ (λ = 0.71073)	MoK$_\alpha$ (λ = 0.71073)
Crystal system	Monoclinic	Monoclinic
Space group	C2/c	P2$_1$/c
***a* (Å)**	60.991(12)	17.703(10)
***b* (Å)**	7.6857(18)	7.556(3)
***c* (Å)**	5.7799(13)	12.385(5)
α(°)	90	90
β(°)	92.122(16)	106.60(3)
γ(°)	90	90
Crystal size (mm)	0.12 × 0.04 × 0.03	0.25 × 0.22 × 0.08
***V* (Å^3)**	2707.5(10)	1587.6(13)
Z	4	2
ρ_{calcd} (g. cm^{-3})	1.209	1.232
μ (mm^{-1})	0.221	0.199
***F*(000)**	1056	624.0
2Θ range for data collection (°)	4.01 to 49.98	5.902 to 50.026
h*/*k*/*l	$-72 \leq h \leq 71$, $-9 \leq k \leq 8$, $-6 \leq l \leq 6$	$-12 \leq h \leq 21$, $-5 \leq k \leq 8$, $-14 \leq l \leq 13$
Reflections collected	9352	6702
Independent reflections	2264 [R_{int} = 0.1058, R_{sigma} = 0.1037]	2755 [R_{int} = 0.0913, R_{sigma} = 0.1648]
Data/restraints/parameters	2264/12/156	0.75/-0.55
Goodness-of-fit on *F*^{2} (S)	1.743	0.964
Final *R* indices [$I > 2\sigma(I)$]	R_1 = 0.1840, wR_2 = 0.4296	R_1 = 0.0805, wR_2 = 0.1969
***R* indices (all data)**	R_1 = 0.2107, wR_2 = 0.4418	R_1 = 0.1855, wR_2 = 0.2513
Largest diff. peak and hole (e.Å^{-3})	1.14/-0.89	0.75/-0.55

REFERENCES

1 G. M. Sheldrick, *Acta Crystallogr. Sect. A Found. Crystallogr.*, 2015, **71**, 3–8.

2 G. M. Sheldrick, *Acta Crystallogr. Sect. C Struct. Chem.*, 2015, **71**, 3–8.

3 O. V. Dolomanov, L. J. Bourhis, R. J. Gildea, J. A. K. Howard and H. Puschmann, *J. Appl. Crystallogr.*, 2009, **42**, 339–341.

4 A. L. Spek, *Acta Crystallogr. Sect. D Biol. Crystallogr.*, 2009, **65**, 148–155.

5 C. F. Macrae, P. R. Edgington, P. McCabe, E. Pidcock, G. P. Shields, R. Taylor, M. Towler and J. Van De Streek, *J. Appl. Crystallogr.*, 2006, **39**, 453–457.